Exciton decay through plasmon modes in planar metal-semiconductor structures

M. V. Durnev*
Spin Optics Laboratory, St. Petersburg State University, 198504 St. Petersburg, Russia and
Ioffe Physical-Technical Institute of the Russian Academy of Sciences, 194021 St. Petersburg, Russia

A. V. Kavokin
Spin Optics Laboratory, St. Petersburg State University, 198504 St. Petersburg, Russia,
Physics and Astronomy School, University of Southampton, Highfield, Southampton SO171BJ, England, United Kingdom, and
Centre National de la Recherche Scientifique, Université Montpellier, Laboratoire Charles Coulomb UMR 5221, F-34095 Montpellier, France

B. Gil
Centre National de la Recherche Scientifique, Université Montpellier, Laboratoire Charles Coulomb UMR 5221, F-34095 Montpellier, France

(Received 15 September 2012; revised manuscript received 19 March 2013; published 16 May 2013)

We develop a nonlocal dielectric-response theory to describe the temperature dependence of exciton lifetime in metal-semiconductor heterostructures. Coupling between excitons and surface plasmons results in a strongly nonmonotonous behavior of exciton decay rate versus temperature, affected by surface plasmons on both sides of the metal layer. Unlike the photons, surface plasmons are not able to escape the sample; hence, the additional decay channel for excitons appears solely due to the plasmon scattering in metal and metal-dielectric interfaces. Tuning the plasmon frequency, one can control the exciton lifetime and under certain conditions emission efficiency.

DOI: 10.1103/PhysRevB.87.195429 PACS number(s): 73.20.Mf, 73.21.Fg

I. INTRODUCTION

Placing a light source near a metal surface can lead to both spontaneous emission enhancement and quenching, depending on the distance between emitter and metal as well as the size and shape of the metal object.[1–5] In the spectral range in which the dielectric function of metal exhibits features linked to collective oscillations of an electron gas, the modification of radiative and nonradiative lifetime contributes to the resonant energy transfer from an emitting dipole to plasmon modes.[6–9] Initially studied for single emitting molecules, the effect is now on topic for use in solid-state physics, especially in gallium-nitride-based light-emitting devices, for which increasing the emission efficiency is one of the major technological challenges. The reduction of exciton lifetime in GaN-InGaN emitters covered by metal layers was observed experimentally in the early 2000s.[10–14] A similar effect has been detected recently in the structures containing metallic nanoparticles[15,16] and cells.[17] More recently, Lu *et al.* coupled the silver plasmon oscillator to the oscillator of a core shell GaN-InGaN nanorod low-dimensional system and observed surface-plasmon lasing.[18] A strong exciton-plasmon coupling regime was recently observed for excitons in GaAs-AlGaAs heterostructures[19] and in CdSe nanocrystals[20] placed near a silver film.

Energies of bulk plasmons in typical metals lie in the ultraviolet spectral range (∼10 eV).[21] However, the introduction of a boundary between the metal and dielectric medium results in the appearance of a new type of coupled light-electronic mode: surface-plasmon polaritons (SPPs) whose resonance frequencies may be found in the near ultraviolet or even optical spectral region.[22] Tuning the SPP frequencies to the vicinity of the band-gap frequency in metal-semiconductor structures allows for coupling of semiconductor emission to the plasmonic modes, resulting in a strong modification of the emitter characteristics. The present theoretical model of exciton coupling to plasmon modes on a planar metal-semiconductor interface[10] is based on a quantum electrodynamic approach, while, to our knowledge, a simpler nonlocal response approach as well as temperature effects have not been considered yet.

Here, by means of a nonlocal dielectric-response theory, we describe the temperature dependence of exciton lifetime in planar metal-semiconductor heterostructures. We show that the exciton nonradiative decay affected by the coupling with surface-plasmon modes on both metal-dielectric interfaces experiences a strong nonmonotonous variation with temperature. Controlling both the plasmon and exciton frequencies [by variation of quantum well (QW) width and composition of barrier layer], one can achieve a significant (up to one order of magnitude) reduction of the exciton lifetime. Although the process of the energy transfer from exciton to plasmon modes is purely nonradiative, the scattering of the surface plasmon on imperfections of metal-dielectric interfaces may result in emission of a photon, therefore giving rise to a radiative channel and the emission enhancement. The interplay between these "radiative" events and the heat dissipation within the metal layer can explain the uncertainty in experimental results claiming emission enhancement as well as quenching for the excitons in planar heterostructures covered by metal layers (see Refs. 10 and 13 for comparison).

This paper is organized as follows: Sec. II contains the analysis of the temperature dependence of exciton radiative lifetime in a quantum well without a metal layer; in Sec. III we discuss the possibility of exciton decay through plasmon modes in a structure covered by a metal layer; Sec. III A represents the nonlocal dielectric-response theory of the exciton coupled to the plasmon on a single metal interface; and in Sec. III B this theory is extended for the case of two metal interfaces. Section IV contains a presentation and discussion of obtained results.

II. EXCITON RADIATIVE LIFETIME IN A QUANTUM WELL

Let us first consider free excitons in a quantum well with a broad thermal distribution of energies (this model is well applicable for light-emitting diode devices, in which the charge carriers are injected in an active region electrically). The excitons therefore have in-plane wave vectors $k_\parallel$ varying in large limits with the corresponding occupation numbers obeying the Boltzmann statistic. Optical selection rules require conservation of the in-plane wave vector for light emitted by excitons in QWs. Light emitted by excitons propagates inside the barrier layers and either escapes the system through its boundary or excites one of the plasmon modes or, after a reflection act, comes back to the QW and eventually decays in the substrate material. It is well known that only the photons with wave vectors inside the so-called light cone can escape the ideal planar sample. Thus, only the excitons with the wave vectors satisfying the condition $k_\parallel < \omega/c$, where ω is the light frequency and c is the speed of light in vacuum, are directly coupled to the continuum of photonic states in vacuum. The decay rate of these excitons depends on the polarization of light.[23]

The integrated decay rate of the thermal population of excitons in a quantum well can be obtained by simply averaging single exciton decays over all values of $k_\parallel < \omega/c$. Considering isotropic isoenergetic contours of an exciton in $k_\parallel$ space and a Boltzmann statistic for the excitons at temperature T, one can obtain[24]

$$\Gamma(T) = \frac{\hbar^2}{Mk_BT}\sum_{i=s,p}\int_0^{\omega/c} k_\parallel dk_\parallel \exp\left(-\frac{\hbar^2 k_\parallel^2}{2Mk_BT}\right)\Gamma_{0,i}(k_\parallel), \tag{1}$$

where $M = m_{e,\parallel} + m_{hh,\parallel}$ is the exciton translation mass; k_B is the Boltzmann constant; $\hbar$ is the Planck constant; $i = s, p$; and $\Gamma_{0,s}(k_\parallel)$ and $\Gamma_{0,p}(k_\parallel)$ are radiative decay rates of s- and p-polarized excitons. For the s-polarized excitons (the polarization vector is oriented in the direction perpendicular to the wave vector), the radiative decay rate increases with $k_\parallel$ as[25]

$$\Gamma_{0,s}(k_\parallel) = \frac{\Gamma_0}{\sqrt{1-(ck_\parallel)^2/(\omega n)^2}}, \tag{2}$$

where ω is the photon frequency, n is the background refractive index, and Γ_0 is the exciton radiative decay rate at $k_\parallel = 0$. For the excitons polarized along the wave vector, (p polarization), the radiative decay rate reads[25]

$$\Gamma_{0,p}(k_\parallel) = \Gamma_0\sqrt{1-(ck_\parallel)^2/(\omega n)^2}. \tag{3}$$

The heavy-hole excitons in zinc-blend-based semiconductor heterostructures as well as A excitons in GaN-InGaN systems are optically inactive in polarization $\boldsymbol{e} \parallel x$,[23] where x is the growth direction, so that the corresponding contribution in p-polarized emission vanishes.

Following Ref. 23, parameter Γ_0 can be expressed via the Bohr radius in the bulk a_B, the excitonic longitudinal transverse splitting pulsation ω_{LT}, and the exciton-photon overlap integral as

$$\Gamma_0 = \frac{n\omega}{2c}\omega_{\mathrm{LT}}\pi a_B^3\left[\int \Phi(x)\cos\left(\frac{n\omega}{c}x\right)dx\right]^2. \tag{4}$$

Here, $\Phi(x)$ is the exciton envelope at the coinciding coordinates of the electron and hole, which in the case of a strong confinement in the x direction can be taken as

$$\Phi(x) = \varphi_{eh}(\boldsymbol{\rho}=0)f_e(x)f_h(x), \tag{5}$$

where $\varphi_{eh}(\boldsymbol{\rho}) = 2\sqrt{2}/(\pi a_B)\mathrm{e}^{-2\rho/a_B}$ is the in-plane wave function of the Coulomb coupled electron and hole, with $\boldsymbol{\rho}$ being the vector of their relative position and $f_{e,h}(x)$ the sized quantized envelopes of the electron and hole in the x direction. For GaN parameters, we obtain $\hbar\omega_{\mathrm{LT}} \approx 1.9$ meV, which for the GaN-$In_{0.2}Ga_{0.8}N$ 4-nm-thick quantum well gives $\hbar\Gamma_0 \approx 0.9$ meV. The corresponding radiative decay time of a single exciton $\tau_0 = 1/(2\Gamma_0) = 0.4$ ps. The parameters used are $m_{e,\parallel} = m_{e,\perp} = 0.2$; $m_{hh,\parallel} = 1.7$; $m_{hh,\perp} = 1.1$[26] (here index $\parallel$ corresponds to the motion in the plane of the quantum well, while $\perp$ stands for the growth direction); $n = 2.47$;[27] and $a_B = 2.8$ nm.[28]

Using Eqs. (2) and (3), the temperature-averaged decay rate Eq. (1) can be written as follows:

$$\begin{aligned}
\Gamma(T) &= \Gamma_s(T) + \Gamma_p(T),\\
\Gamma_s(T) &= 2\Gamma_0\sqrt{\alpha}[n\mathcal{F}(\sqrt{\alpha}n) - n\mathrm{e}^{-\alpha}\mathcal{F}(\sqrt{\alpha(n^2-1)})],\\
\Gamma_p(T) &= \Gamma_0\left[1 - \frac{\mathrm{e}^{-\alpha}\sqrt{n^2-1}}{n} - \frac{\mathcal{F}(\sqrt{\alpha}n)}{\sqrt{\alpha}n}\right.\\
&\quad\left. + \frac{\mathrm{e}^{-\alpha}\mathcal{F}(\sqrt{\alpha(n^2-1)})}{\sqrt{\alpha}n}\right].
\end{aligned} \tag{6}$$

Here, $\alpha = \hbar^2\omega^2/(2Mc^2k_BT)$ is the ratio of the exciton kinetic energy at the boundary of the light cone to the thermal energy and $\mathcal{F}(x)$ is defined as $\mathcal{F}(x) = \mathrm{e}^{-x^2}\int_0^x \mathrm{e}^{t^2}dt$. Parameter α can be rewritten as $\alpha = T_0/T$, where characteristic temperature T_0 for the exciton in GaN is $T_0 \approx 0.07$ K. Therefore, in a reasonable experimental range of temperatures, parameter $\alpha \ll 1$. In this case, following Eq. (6) one obtains for the exciton radiative lifetime $\tau = 1/(2\Gamma)$

$$\frac{\tau}{\tau_0} = \frac{3}{2}\frac{n}{4n^3 + (1-4n^2)\sqrt{n^2-1}}\frac{T}{T_0}, \tag{7}$$

which yields linear temperature increase.

III. EXCITON COUPLING TO THE SURFACE-PLASMON MODES

Surface plasmons propagate along a metal-dielectric interface with wave vectors β exceeding ω/c, which is why the amplitude of the electromagnetic field of a plasmon decays in both directions perpendicular to the metal surface. The dispersion of these modes is given by[29]

$$\beta^2 = \frac{\varepsilon_S\varepsilon_M(\omega)}{\varepsilon_S + \varepsilon_M(\omega)}\frac{\omega^2}{c^2}, \tag{8}$$

where $\varepsilon_{S,M}$ are dielectric functions of the semiconductor (dielectric) and metal, respectively. The electric field of a plasmon mode decays exponentially inside the semiconductor

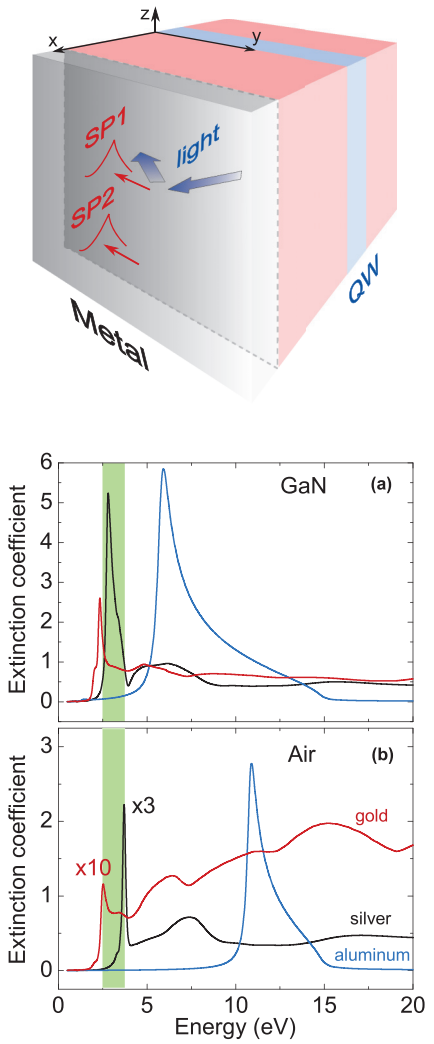

FIG. 1. (Color online) Schematic illustration of the structure (top) and imaginary parts of the effective dielectric function Eq. (8) (bottom) for different metals and values of ε_S. (a) $\varepsilon_S = 6.1$, corresponding to GaN. (b) $\varepsilon_S = 1$. The green area presents the typical range of exciton energies in the InGaN quantum well.

with a penetration depth

$$l_S = \frac{c}{\omega}\sqrt{\frac{-(\varepsilon_S + \varepsilon_M)}{\varepsilon_S^2}} \tag{9}$$

and inside the metal with a depth

$$l_M = \frac{c}{\omega}\sqrt{\frac{-(\varepsilon_S + \varepsilon_M)}{\varepsilon_M^2}}. \tag{10}$$

The frequency dependence of ε_M in real metals is quite complicated. ε_M has a large imaginary part accounting for the absorption of light in metal. The useful characteristic of a plasmon is the extinction coefficient, defined as the imaginary part of the effective dielectric function in the right part of Eq. (8). The frequency dependence of the extinction coefficient at the interfaces with air ($\varepsilon_S = 1$) and GaN ($\varepsilon_S = 6.1$)[27] for aluminum, silver, and gold [experimental data on $\varepsilon_M(\omega)$ taken from Refs. 30–32] is presented in the lower panel of Fig. 1. For ease of comparison, the range of exciton energies in InGaN with indium concentration varying from 0 to 0.3 is shown in green. One can see that the most effective plasmon generation on both interfaces can be performed with the use of the aluminum layer, but its plasmon peak is quite far from the attractive range of frequencies. The gold peak is close to that range, but the losses are too large to provide an effective coupling, so we stop at the silver coating and use its parameters for the following simulations.

We will consider in this paper the structure schematically shown in the upper panel of Fig. 1. It consists of a quantum well (QW) sandwiched between two barrier layers, one of them covered by a metal film. The direction of growth is labeled by x; we will denote the thickness of the metal layer as d, the width of the well as a, and the position of its center with respect to the metal-barrier interface as x_{QW}. The fundamental property of a smooth metal-semiconductor interface is that neither the metal-semiconductor plasmon mode (SP1) nor the metal-air mode (SP2) can be excited by the photons with $k_\parallel < \omega/c$. However, the photons outside the light cone with $\omega/c < k_\parallel < n\omega/c$, though unable to escape the sample, may contribute to the excitation of the SP2 mode. This leaky mode propagating on the metal-air interface can be excited due to the exponential tail of its electric field, which penetrates into the semiconductor region.[22,29] In addition, as we will show below, the exciton can decay directly into the plasmon modes even at $k_\parallel > \omega/c$ for SP1 and $k_\parallel > n\omega/c$ for SP2 provided *solely* by the nonzero imaginary part of the dielectric function of metal. These additional plasmon-assisted exciton decay channels can be taken into account in a nonlocal dielectric-response approach with the coupling provided by the electric interaction between exciton dipole momentum and the in-plane component of the plasmon field.

A. Single metal-semiconductor interface

Let us first consider two semi-infinite media: a metal and semiconductor occupying $x < 0$ and >0 regions, respectively. The presence of metal modifies both radiative and nonradiative lifetimes of an exciton in the quantum well situated in the semiconductor region. We will be interested in TM modes with three nonzero components of the electromagnetic field, H_y, E_x, and E_z. Considering heavy-hole excitons in a polar oriented wurtzite quantum well, only the optical transitions with a polarization vector lying in the plane of the well are allowed. Therefore, we will be interested in the E_z component of the electric field, the wave equation for which reads

$$\frac{\partial^2 E_z}{\partial x^2} - \varkappa^2(x) E_z = 4\pi \frac{\varkappa^2(x)}{\varepsilon(x)} P_z, \tag{11}$$

where $\varkappa^2(x) = \beta^2 - \varepsilon(x)\omega^2/c^2$, β is the in-plane wave vector of the wave ($E_{x,z} \propto e^{i\beta_y y + i\beta_z z}$), P_z is the excitonic polarization in the quantum well, and

$$\varepsilon(x) = \begin{cases} \varepsilon_M, & x < 0 \\ \varepsilon_S, & x > 0 \end{cases}.$$

For $\mathrm{Re}(\varkappa^2) > 0$, Eq. (11) describes evanescent at $x \to \pm\infty$ waves corresponding to surface plasmons propagating with wave vector β. To obtain solutions of Eq. (11), we will use the Green's-function technique;[23] the Green's function $G(x,x')$

satisfies the following equation:

$$\frac{\partial^2 G}{\partial x^2} - \varkappa^2(x)G = \delta(x - x'). \tag{12}$$

The boundary conditions for the Green's function at $x = 0$ should be set the same as for electric field:

$$\begin{aligned} G|_{x\to 0+} &= G|_{x\to 0-}, \\ \frac{\varepsilon(x)}{\varkappa^2(x)}\frac{\partial G}{\partial x}\bigg|_{x\to 0+} &= \frac{\varepsilon(x)}{\varkappa^2(x)}\frac{\partial G}{\partial x}\bigg|_{x\to 0-}. \end{aligned} \tag{13}$$

We will further restrict ourselves to the case of $x' > 0$ only, because the quantum well is situated in the semiconductor region. We will also neglect the dielectric contrast between the quantum well and barrier materials. The solution of Eq. (12) can therefore be written as follows:

$$\begin{aligned} G(x,x') = \frac{1}{2\varkappa_S}\left(1 - \frac{2\varepsilon_S\varkappa_M}{\varepsilon_S\varkappa_M + \varepsilon_M\varkappa_S}\right)\mathrm{e}^{-\varkappa_S(x+x')} \\ - \frac{1}{2\varkappa_S}\mathrm{e}^{-\varkappa_S|x-x'|}, \quad x > 0, \end{aligned} \tag{14}$$

and

$$G(x,x') = -\frac{1}{\varkappa_S}\frac{\varepsilon_S\varkappa_M}{\varepsilon_S\varkappa_M + \varepsilon_M\varkappa_S}\mathrm{e}^{\varkappa_M x - \varkappa_S x'}, \quad x < 0, \tag{15}$$

where $\varkappa_{M,S}$ are $\varkappa(x)$ at $x < 0$ and >0, respectively. Note that the Green's function for $x > 0$ comprises two terms: the bulk one (the second term) and the interface one (the first term). It should be also noted that the two poles of the Green's function correspond to (1) the bulk wave in the semiconductor region propagating in the lateral direction and (2) the interface state (surface plasmon) with the related dispersion $\beta(\omega)$ [see Eq. (8)].

The solution of wave equation (11) can now be written as

$$E_z(x) = E_z^{(0)}(x) + 4\pi\int_{-\infty}^{+\infty}\frac{\varkappa^2(x')}{\varepsilon(x')}P_z(x')G(x,x')dx', \tag{16}$$

where $E_z^{(0)}$ is the solution corresponding to $P_z = 0$. The dielectric response of the exciton is[23]

$$\begin{aligned} 4\pi P_z(x) &= g(\omega)\Phi(x)\int\Phi(x')E_z(x')dx', \\ g(\omega) &= \frac{\pi a_B^3\varepsilon_S\omega_{\mathrm{LT}}}{\omega_0 - \omega - i\Gamma}, \end{aligned} \tag{17}$$

where ω_0 is the exciton resonant frequency and Γ its nonradiative decay rate. We will restrict ourselves to a strong exciton confinement in the x direction (which is generally a good approximation for InGaN-GaN wells), so that [see Eq. (5)] in the infinite barrier approach

$$\Phi(x) = \frac{4\sqrt{2}}{\pi a_B a}\cos^2\frac{\pi}{a}(x - x_{\mathrm{QW}}),$$

where a is the well width and x_{QW} is the coordinate of the well center. Combining Eqs. (16) and (17), we obtain for the electric field

$$E_z(x) = E_z^{(0)}(x) + g(\omega)\Lambda\int\frac{\varkappa_S^2}{\varepsilon_S}\Phi(x')G(x,x')dx', \tag{18}$$

where the limits of integration are set to the quantum well region ($x_{\mathrm{QW}} - a/2 \leqslant x \leqslant x_{\mathrm{QW}} + a/2$) and

$$\begin{aligned} \Lambda &= \int\Phi(x)E_z(x)dx = \frac{\int\Phi(x)E_z^{(0)}(x)dx}{1 - g(\omega)I}, \\ I &= \frac{\varkappa_S^2}{\varepsilon_S}\int\int dxdx'\Phi(x')\Phi(x)G(x,x'). \end{aligned} \tag{19}$$

After further transformations, Λ can be written as

$$\Lambda = \frac{\omega_0 - \omega - i\Gamma}{\omega_0 - i\Gamma - \delta\omega - \omega}\int\Phi(x)E_z^{(0)}(x)dx, \tag{20}$$

where $\delta\omega$ is the renormalization of the exciton complex frequency $\omega_0 - i\Gamma$ comprising the frequency shift (real part) and the radiative decay rate to the electromagnetic modes (imaginary part):[23,33]

$$\begin{aligned} \delta\omega = \frac{1}{2}\pi a_B^3\omega_{\mathrm{LT}}\varkappa_S\left\{\frac{\varepsilon_M\varkappa_S - \varepsilon_S\varkappa_M}{\varepsilon_S\varkappa_M + \varepsilon_M\varkappa_S}\left[\int\Phi(x)\mathrm{e}^{-\varkappa_S x}dx\right]^2\right. \\ \left. - \int dxdx'\Phi(x)\Phi(x')\mathrm{e}^{-\varkappa_S|x-x'|}\right\}. \end{aligned} \tag{21}$$

The real part of $\delta\omega$ gives an insignificant shift of the resonant exciton frequency, while we are interested mostly in its imaginary part, which gives an additional decay channel.

Let us stress that in the case of evanescent waves [$\mathrm{Re}(\varkappa_S) > 0$] the only imaginary contribution to $\delta\omega$ arises from the imaginary part of the dielectric function of the metal, $\varepsilon_M(\omega)$, setting the finite lifetime of the surface plasmon. In the idealized case when the surface plasmon freely propagates along the metal-dielectric interface without decay, exciton interaction with it reduces only to the radiative shift of the exciton frequency and no additional emission channel arises. This case is opposite to the emission of a photon, since the photon has an additional degree of freedom in the x direction allowing it to finally escape the sample. The dielectric function of the metal can be written as $\varepsilon_M(\omega) = \varepsilon'_M(\omega) + i\varepsilon''_M(\omega)$, with two components known from experimental data (see Fig. 1). The standard Drude model, on the other hand, in the frequency region where losses are relatively low, which is actually of interest for us, gives

$$\varepsilon'_M(\omega) = 1 - \frac{\omega_p^2}{\omega^2}, \quad \varepsilon''_M(\omega) = \frac{\gamma\omega_p^2}{\omega^3}, \tag{22}$$

with ω_p being the bulk-plasmon frequency and γ the internal losses in the metal. External losses γ_{ext} such as scattering on interface roughness and on boundaries of the sample can be included in $\varepsilon''_M(\omega)$ as additional term $\gamma_{\mathrm{ext}}\omega_p^2/\omega^3$.

Let us now turn back to Eq. (21). For simplicity, we consider a thin quantum well so that the electric field can be taken as uniform inside it (this is reasonable in the case of large-field penetration length so that $\varkappa_S a \ll 1$, which is always fulfilled for GaN). In the case of evanescent waves ($\beta > \sqrt{\varepsilon_S}\omega/c$), we then obtain for the exciton nonradiative decay $\Gamma_{0,\mathrm{SP}} \equiv \mathrm{Im}(\delta\omega)$

through the plasmon modes:

$$\Gamma_{0,\mathrm{SP}} = \frac{4}{\pi}\omega_{\mathrm{LT}}\varkappa_S a_B \mathrm{Im}\left(\frac{\varepsilon_M\varkappa_S - \varepsilon_S\varkappa_M}{\varepsilon_S\varkappa_M + \varepsilon_M\varkappa_S}\right)\mathrm{e}^{-2\varkappa_S x_{\mathrm{QW}}}. \quad (23)$$

Equation (21) also describes radiative decay into the photon modes ($\beta < \sqrt{\varepsilon_S}\omega/c$) if one makes the substitution $\varkappa_S \to -ik_S$, arriving for $\Gamma_0 \equiv \mathrm{Im}(\delta\omega)$ at

$$\Gamma_0 = \frac{1}{2}\pi a_B^3\omega_{\mathrm{LT}}k_S\left[\int_{-a/2}^{a/2} dx\,\Phi(x+x_{\mathrm{QW}})\cos k_S x\right]^2 \times\left[1+\mathrm{Re}\left\{\mathrm{e}^{i2k_S x_{\mathrm{QW}}}\frac{\varepsilon_S\varkappa_M + i\varepsilon_M k_S}{\varepsilon_S\varkappa_M - i\varepsilon_M k_S}\right\}\right]. \quad (24)$$

One can see that Γ_0 in the presence of the metal-semiconductor interface differs from the one in the uniform semiconductor medium [cf. Eq. (4)] by the second term in square brackets of Eq. (24); this modification of radiative decay can be referred to as the Purcell effect (see, for instance, Ref. 34 for the same effect analyzed for an electric dipole placed in a metal sphere). $\Gamma_{0,\mathrm{SP}}$ and the modification of Γ_0 have the same sense as discussed in Ref. 2, nonradiative and radiative decays of a dipole placed near a metal nanosphere. In the case of the thin well ($k_S a \ll 1$), one obtains

$$\Gamma_0 = \frac{4}{\pi}\omega_{\mathrm{LT}}k_S a_B\left[1+\mathrm{Re}\left(\mathrm{e}^{i2k_S x_{\mathrm{QW}}}\frac{\varepsilon_S\varkappa_M + i\varepsilon_M k_S}{\varepsilon_S\varkappa_M - i\varepsilon_M k_S}\right)\right]. \quad (25)$$

The set of Eqs. (20), (21), and (23) can be understood in another interesting way. We can use the fact that the denominator $\varepsilon_S\varkappa_M + \varepsilon_M\varkappa_S$ becomes zero at frequencies corresponding to surface-plasmon dispersion Eq. (8), so that in the vicinity of such frequency it can be expanded to the linear at $\omega - \omega_{\mathrm{SP}}(\beta)$ term. Therefore, setting the denominator of Eq. (20) equal to zero at the complex frequency domain, after neglecting the unimportant frequency shifts, we obtain

$$(\omega - \omega_0 + i\Gamma)(\omega - \omega_{\mathrm{SP}} + i\gamma) - \Omega^2 = 0, \quad (26)$$

where $\omega_{\mathrm{SP}}(\beta) - i\gamma(\beta)$ is the complex frequency of the surface plasmon (γ can also contain the terms due to external losses) and Ω is the coupling term:

$$\Omega^2 = \frac{8}{\pi}\varkappa_S a_B\omega_{\mathrm{LT}}\omega_0\frac{\varepsilon_S|\varepsilon'_M|}{|\varepsilon'_M|^2 - \varepsilon_S^2}\mathrm{e}^{-2\varkappa_S x_{\mathrm{QW}}}. \quad (27)$$

Equation (26) describes the system of two coupled oscillators,[19] the exciton and surface plasmon, and in the resonance regime ($\omega_0 = \omega_{\mathrm{SP}}$) it has the two following solutions:

$$\omega_\pm = \omega_0 - i\frac{\Gamma+\gamma}{2} \pm \sqrt{\Omega^2 - \left(\frac{\Gamma-\gamma}{2}\right)^2}, \quad (28)$$

with imaginary parts giving the modified decay rates due to the intermixing between two oscillatory modes. For the GaN parameters (see Sec. II), the dielectric function of silver and the set $\hbar\omega_0 = 2.4$ eV, $\beta = 0.05$ nm^{-1}, and x_{QW}, the coupling parameter $\hbar\Omega \approx 25$ meV, which is well correlated with experimental results for the strongly coupled exciton-plasmon systems (see Refs. 19 and 20).

B. Metal layer between two dielectric media

Let us consider now a more realistic, from the experimental point of view, "air-metal layer-semiconductor" structure. Let us denote the thickness of the layer as d and the dielectric constant of air ε_0 ($\varepsilon_0 = 1$); the metal-semiconductor interface is situated at $x = 0$ as before, so that the coordinate of the metal-air interface is $x = -d$. Now, when we have two metal-dielectric interfaces both metal-semiconductor (SP1) and metal-air (SP2) plasmon modes are present and the coupling between them leads to the modification of the dispersion law and to the appearance of mixed-symmetric and antisymmetric modes.[22,29] The exciton decay through mixed modes can be found in the same manner as for a single interface; for that purpose, one should obtain the Green's function of Eq. (11) with the additional boundary conditions [Eq. (13)] at $x = -d$. This procedure gives for $G(x,x')$ at $x > 0, x' > 0$

$$G(x,x') = -\frac{1}{2\varkappa_S}\mathrm{e}^{-\varkappa_S|x-x'|} - \frac{1}{2\varkappa_S}F(\varkappa_0,\varkappa_M,\varkappa_S)\mathrm{e}^{-\varkappa_S(x+x')},$$
$$F(\varkappa_0,\varkappa_M,\varkappa_S) = \frac{(\varkappa_M\varepsilon_0 + \varkappa_0\varepsilon_M)(\varkappa_M\varepsilon_S - \varkappa_S\varepsilon_M) - \mathrm{e}^{-2\varkappa_M d}(\varkappa_M\varepsilon_0 - \varkappa_0\varepsilon_M)(\varkappa_M\varepsilon_S + \varkappa_S\varepsilon_M)}{(\varkappa_M\varepsilon_0 + \varkappa_0\varepsilon_M)(\varkappa_M\varepsilon_S + \varkappa_S\varepsilon_M) - \mathrm{e}^{-2\varkappa_M d}(\varkappa_M\varepsilon_0 - \varkappa_0\varepsilon_M)(\varkappa_M\varepsilon_S - \varkappa_S\varepsilon_M)}\mathrm{e}^{-\varkappa_S(x+x')}. \quad (29)$$

Let us note that as before the second pole of $G(x,x')$ corresponds to the surface-mode solutions, this time two coupled plasmons. The strength of coupling is given by the $\mathrm{e}^{-2\varkappa_M d}$ term, dependent on the metal layer thickness. The renormalization of the exciton frequency is now given by [cf. Eq. (21)]

$$\delta\omega = -\frac{1}{2}\pi a_B^3\omega_{\mathrm{LT}}\varkappa_S\left\{F(\varkappa_0,\varkappa_M,\varkappa_S)\left[\int\Phi(x)\mathrm{e}^{-\varkappa_S x}dx\right]^2 + \int dx dx'\Phi(x)\Phi(x')\mathrm{e}^{-\varkappa_S|x-x'|}\right\}. \quad (30)$$

The radiative decay due to the photon modes corresponds to $\beta < \omega/c$ (when none of the surface modes are present) and can be written as [cf. Eq. (24)]

$$\Gamma_0 = \frac{4}{\pi}\omega_{\mathrm{LT}}k_S a_B\{1+\mathrm{Re}[\mathrm{e}^{i2k_S x_{\mathrm{QW}}}F(-ik_0,\varkappa_M,-ik_S)]\}. \quad (31)$$

As for the decay rate through the plasmon modes, the two cases should be distinguished: (1) $\omega/c < \beta < \sqrt{\varepsilon_S}\omega/c$ and (2) $\beta > \sqrt{\varepsilon_S}\omega/c$. The first case corresponds to the so-called "leaky" plasmon mode when the metal-air plasmon and a photon in the semiconductor coexist. The second one describes two coupled

plasmons. Thus, the decay through plasmon modes should be written separately for those cases so that for case 1

$$\Gamma^{(1)}_{0,\mathrm{SP}} = \frac{4}{\pi}\omega_{\mathrm{LT}} k_S a_B \{1 + \mathrm{Re}[e^{i2k_S x_{\mathrm{QW}}} F(\varkappa_0, \varkappa_M, -ik_S)]\} \tag{32}$$

and for case 2

$$\Gamma^{(2)}_{0,\mathrm{SP}} = -\frac{4}{\pi}\omega_{\mathrm{LT}} \varkappa_S a_B \mathrm{Im}[F(\varkappa_0, \varkappa_M, \varkappa_S)] e^{-2\varkappa_S x_{\mathrm{QW}}}. \tag{33}$$

Equations (31)–(33) give the total decay rate of a single exciton to the photon and both surface-plasmon modes for all values of exciton wave vector β, which we will denote by $\Gamma_{\mathrm{tot}}(\beta)$. The calculation of the integrated exciton decay rate as a function of temperature can be obtained in a manner similar to Eq. (1) by averaging the decay of a single exciton:

$$\Gamma(T) = \frac{\hbar^2}{Mk_BT}\int_0^\infty \beta d\beta \exp\left(-\frac{\hbar^2\beta^2}{2Mk_BT}\right)\Gamma_{\mathrm{tot}}(\beta). \tag{34}$$

IV. RESULTS

Figure 2 presents the results of calculations of the exciton total decay rate in structures with single [Fig. 2(c)] and double [Fig. 2(d)] metal-dielectric interfaces. For clarity, Fig. 2(a) depicts the dispersion curves of the surface plasmon bound to air and the GaN bulk semiconductor calculated accounting for intrinsic metal losses. Different curves in Figs. 2(c) and 2(d) correspond to different exciton resonant frequencies $\hbar\omega_0$ varying in the range of 2 to 2.8 eV. One can see that the spectra exhibit a well-defined peak at the wave vector corresponding to exciton-plasmon resonance on the GaN side (SP1 mode). With the increase of exciton frequency, the peak broadens and finally vanishes in the frequency region where metal losses become noticeable [see Fig. 2(a)]. The detailed shape of the decay spectra at $\hbar\omega_0 = 2.4$ eV is presented in Fig. 2(b) for different metal thicknesses. Decrease of the metal layer thickness results in the shift of the peak toward larger wave vectors, which is explained by the decrease of energy of the SP1 plasmon due to the interaction with SP2. Tiny dips at $\beta = \omega/c$ are related to the above-mentioned leaky plasmon mode at the interface with air. It is clearly seen that generally the influence of this plasmon on the final exciton decay is almost negligible.

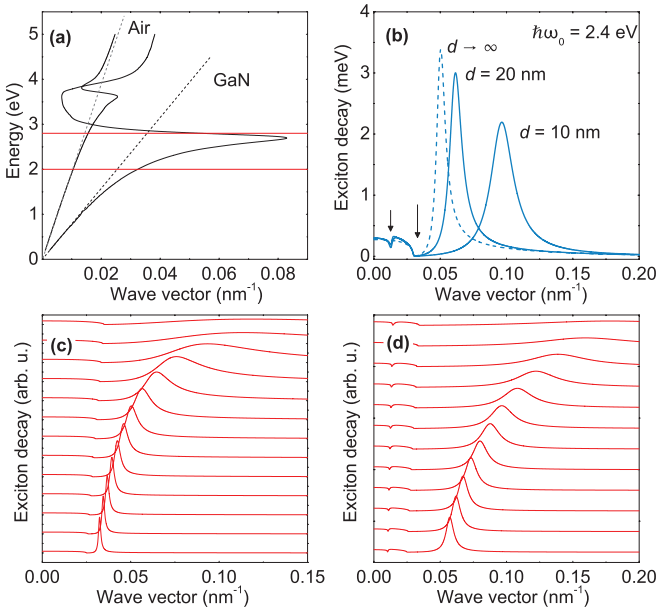

FIG. 2. (Color online) Exciton total decay rate. (a) Dispersion curves of two noninteracting plasmons bound to air and GaN obtained accounting for intrinsic metal losses (see Fig. 1); horizontal lines indicate the energy range from 2 to 2.8 eV. (b) Exciton decay rate as a function of its wave vector at exciton resonance frequency $\hbar\omega_0 =$ 2.4 eV (corresponding to bulk $In_{0.3}Ga_{0.7}N$) for $d = 10$ nm, 20 nm, and ∞ (the single metal-semiconductor interface). (c) Exciton decay rate in the structure with a single metal interface for various $\hbar\omega_0$ ranging from 2 to 2.8 eV. (d) Exciton decay rate in the structure with two metal interfaces for various $\hbar\omega_0$ ranging from 2 to 2.8 eV. In panels (b)–(d) $x_{\mathrm{QW}} = 10$ nm, and in panel (d) $d = 10$ nm. Arrows in panel (b) indicate wave vectors $k = \omega/c$ and $\sqrt{\varepsilon_S}\omega/c$.

To analyze the temperature dependence of exciton decay to the plasmon modes, let us consider Eq. (34) in high-temperature and low-temperature limits (the characteristic temperature defining the boundary between those limits will be discussed later). It is clear that in the high-temperature limit the exponent in the integral can be set to unity, resulting in linear temperature exciton lifetime dependence:

$$\tau = \frac{1}{4\int_0^\infty \eta d\eta \Gamma_{\mathrm{tot}}(\beta_0\eta)}\frac{T}{T_0}, \tag{35}$$

where $\beta_0 = \omega_0/c$ and η is the dimensionless variable. The proportionality coefficient $\partial\tau/\partial T$ is presented in Fig. 3 as a function of exciton frequency ω_0. It is clearly seen that the coefficient is strongly reduced in the vicinity of exciton-plasmon resonance. For comparison, $\partial\tau/\partial T$ neglecting coupling to surface plasmons is found to be [see Eq. (7)] $\approx$1.4 ps/K, meaning the possible reduction of plasmon-induced exciton nonradiative lifetime up to one order of magnitude. We should note that in the region of $\hbar\omega_0 \approx 3.5$ eV our model is no longer valid, because in that region the resonant exciton transitions in the GaN barrier layer become apparent, leading to a strong frequency dependence of ε_S.

Let us now turn to a low-temperature region where temperature dependence of the exponential term in Eq. (34)

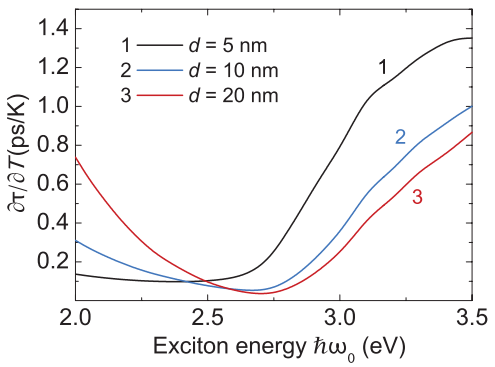

FIG. 3. (Color online) Coefficient $\partial\tau/\partial T$ as a function of exciton energy $\hbar\omega_0$. One can see distinct dips corresponding to exciton-plasmon resonance. For comparison $\partial\tau/\partial T \approx 1.4$ ps/K neglecting plasmon coupling.

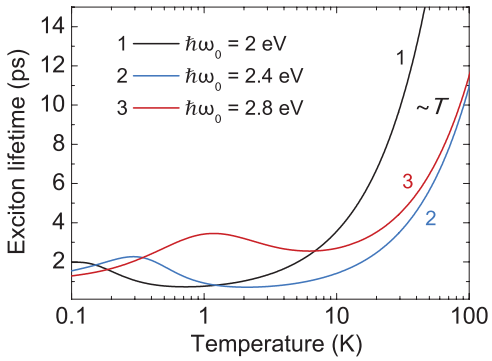

FIG. 4. (Color online) Exciton lifetime as a function of temperature. Different curves correspond to different exciton resonance frequencies. Note that the temperature axis is scaled logarithmically. $d = 10$ nm and $x_{QW} = 10$ nm.

should be taken into account and gives rise to a strongly nonmonotonous behavior of exciton lifetime. The calculated curves are presented in Fig. 4 for different values of ω_0. All curves exhibit dips near the temperature where the maximally populated exciton state in k space [the population is given by $k\exp(-\frac{\hbar^2k^2}{2Mk_BT})$] coincides with the plasmon peak position in $\Gamma_{tot}(k)$. This characteristic temperature (let us denote it by $\tilde{T}_0$) defines the transition to the high-temperature limit, where the lifetime increases linearly with temperature. The dip shifts to the region of higher temperatures with the increase of ω_0 as the plasmon peak shifts to the higher wave-vector values (see Fig. 2). Figure 4 shows that the values of $\tilde{T}_0$ lie in the range of $1\div10$ K, so that nonmonotonous behavior becomes apparent in a wider range of temperatures as compared to the case in which decay to plasmon modes is neglected (i.e., $\tilde{T}_0 \gg T_0$).

V. CONCLUSIONS

In conclusion, we have shown that the coupling of excitons in quantum wells with surface plasmons at metal-semiconductor and metal-air interfaces yields additional channels of exciton nonradiative decay which may significantly reduce the exciton lifetime. Those additional channels are provided *solely* by the nonzero imaginary part of the dielectric function of the metal, reflecting the finite surface-plasmon lifetime. The scattering process of the surface plasmon might be, however, followed by the emission of a photon, giving rise to the radiative decay channel for the exciton. The temperature dependence of exciton lifetime becomes strongly nonmonotonous in the presence of plasmons. It experiences a dip as the exciton gas heats up to the energies of a metal-semiconductor plasmon. The plasmon-controlled emission enhancement opens the way to lifetime engineering in semiconductor-metal quantum confined structures which may be widely used in solid-state light emitters.

ACKNOWLEDGMENTS

We acknowledge support from GANEX (Grant No. ANR-11-LABX-0014). GANEX belongs to the public funded "Investissements d'Avenir" program managed by the French National Research Agency. This work is partly supported by Initial Training Networks "Clermont4" (Grant No. PITNGA-2009-235114) and "Index" (Grant No. FP7-2011-289968) of the 7th Framework Program of the European Community and Russian Ministry of Education and Science (Contract No. 11.G34.31.0067). M. D. acknowledges financial support from the Dynasty Foundation and European Union projects POLAPHEN and SPANGL4Q and thanks M. Glazov for helpful discussions.

*durnev@mail.ioffe.ru

[1] J. Gersten and A. Nitzan, J. Chem. Phys. **75**, 1139 (1981).
[2] H. Mertens, A. F. Koenderink, and A. Polman, Phys. Rev. B **76**, 115123 (2007).
[3] P. Anger, P. Bharadwaj, and L. Novotny, Phys. Rev. Lett. **96**, 113002 (2006).
[4] S. Kühn, U. Håkanson, L. Rogobete, and V. Sandoghdar, Phys. Rev. Lett. **97**, 017402 (2006).
[5] J. N. Farahani, D. W. Pohl, H.-J. Eisler, and B. Hecht, Phys. Rev. Lett. **95**, 017402 (2005).
[6] H. Morawitz and M. R. Philpott, Phys. Rev. B **10**, 4863 (1974).
[7] R. R. Chance, A. Prock, and R. Silbey, Adv. Chem. Phys. **37**, 1 (1978).
[8] G. W. Ford and W. H. Weber, Phys. Rep. **113**, 195 (1984).
[9] J.-H. Song, T. Atay, S. Shi, H. Urabe, and A. V. Nurmikko, Nano Lett. **5**, 1557 (2005).
[10] I. Gontijo, M. Boroditsky, E. Yablonovitch, S. Keller, U. K. Mishra, and S. P. DenBaars, Phys. Rev. B **60**, 11564 (1999).
[11] A. Neogi, C.-W. Lee, H. O. Everitt, T. Kuroda, A. Tackeuchi, and E. Yablonovitch, Phys. Rev. B **66**, 153305 (2002).
[12] K. Okamoto, I. Niki, A. Shvartser, Y. Narukawa, T. Mukai, and A. Scherer, Nat. Mater. **3**, 601 (2004).
[13] K. Okamoto, I. Niki, A. Scherer, Y. Narukawa, T. Mukai, and Y. Kawakami, Appl. Phys. Lett. **87**, 071102 (2005).
[14] J. Lin, A. Mohammadizia, A. Neogi, H. Morkoc, and M. Ohtsu, Appl. Phys. Lett. **97**, 221104 (2010).
[15] L.-W. Jang *et al.*, Opt. Express **20**, 2116 (2012).
[16] A. A. Toropov, T. V. Shubina, V. N. Jmerik, S. V. Ivanov, Y. Ogawa, and F. Minami, Phys. Rev. Lett. **103**, 037403 (2009).
[17] K. Tanaka, E. Plum, J. Y. Ou, T. Uchino, and N. I. Zheludev, Phys. Rev. Lett. **105**, 227403 (2010).
[18] Y.-J. Lu *et al.*, Science **337**, 450 (2012).
[19] J. Bellessa, C. Symonds, C. Meynaud, J. C. Plenet, E. Cambril, A. Miard, L. Ferlazzo, and A. Lemaitre, Phys. Rev. B **78**, 205326 (2008).
[20] D. E. Gómez, K. C. Vernon, P. Mulvaney, and T. J. Davis, Nano Lett. **10**, 274 (2010).
[21] C. Kittel, *Introduction to Solid State Physics* (Wiley, New York, 1995).
[22] S. Maier, *Plasmonics. Fundamentals and Applications* (Springer, New York, 2007).

[23]E. L. Ivchenko, *Optical Spectroscopy of Semiconductor Nanostructures* (Alpha Science, Harrow, 2005).
[24]J. Feldmann, G. Peter, E. O. Göbel, P. Dawson, K. Moore, C. Foxon, and R. J. Elliott, Phys. Rev. Lett. **59**, 2337 (1987).
[25]P. Lefebvre, J. Allègre, B. Gil, A. Kavokine, H. Mathieu, W. Kim, A. Salvador, A. Botchkarev, and H. Morkoç, Phys. Rev. B **57**, R9447 (1998).
[26]S. Khatsevich and D. H. Rich, J. Phys.: Condens. Matter **20**, 215223 (2008).
[27]N. A. Sanford, L. H. Robins, A. V. Davydov, A. Shapiro, D. V. Tsvetkov, A. V. Dmitriev, S. Keller, U. K. Mishra, and S. P. DenBaars, J. Appl. Phys. **94**, 2980 (2003).
[28]P. Ramvall, S. Tanaka, S. Nomura, P. Riblet, and Y. Aoyagi, Appl. Phys. Lett. **73**, 1104 (1998).
[29]J. M. Pitarke, V. M. Silkin, E. V. Chulkov, and P. M. Echenique, Rep. Prog. Phys. **70**, 1 (2007).
[30]H. Ehrenreich and H. Philipp, Phys. Rev. **128**, 1622 (1962).
[31]H. Ehrenreich, H. Philipp, and B. Segall, Phys. Rev. **132**, 1918 (1963).
[32]B. R. Cooper, H. Ehrenreich, and H. R. Philipp, Phys. Rev. **138**, A494 (1965).
[33]A. V. Kavokin and E. L. Ivchenko, Sov. Phys. Solid State **34**, 968 (1992).
[34]M. M. Glazov, E. L. Ivchenko, A. N. Poddubny, and G. Khitrova, Fiz. Tverd. Tela **53**, 1665 (2011).